Multivariate Circulant Singular Spectrum Analysis *

Juan Bógalo
Universidad Autónoma de Madrid
SPAIN

Pilar Poncela
Universidad Autónoma de Madrid
SPAIN

Eva Senra
Universidad de Alcalá
SPAIN

July 16, 2020

Abstract

Multivariate Circulant Singular Spectrum Analysis (M-CiSSA) is a non-parametric automated technique that allows to extract signals of time series at any frequency specified beforehand. It is useful to uncover co-movements at different frequencies and understand their commonalities and specificities. We apply M-CiSSA to understand the main drivers and co-movements of energy commodity prices at trend and cyclical frequencies that are key to assess energy policy at different time horizons. We clearly distinguish the detached behaviour of US natural gas from the rest of energy commodities at both frequencies while coals and Japan natural gas only decouple at the cyclical frequency.

Keywords: Block circulant matrices, multivariate signal extraction, singular spectrum analysis, co-movement, decoupled markets, energy prices

*Financial support from the Spanish government, contract grants MINECO/FEDER ECO2015-70331-C2-1-R, ECO2015-66593-P, ECO2016-76818-C3-3-P, PID2019-107161GB-C32 and PID2019-108079GB-C22 is acknowledged.

1 Introduction

Energy commodities accounted for 40.9% of the world trade between 2014 and 2016, according to IMF data. Energy prices are key for the competitiveness in industry and notably influence the energy prices paid by consumers affecting their energy consumption patterns and total expenditures. In fact, final prices paid by consumers are both affected by movements in commodity markets as well as by policy decisions. The International Energy Agency recognizes [1] that understanding and monitoring the fluctuations in energy prices around the world is of key importance for analysts, investors and policy makers, especially, as countries move away from regulated pricing.

Policy makers aim to modify energy consumer's patterns. Some global international initiatives set their targets towards transforming the society and the economy into a more sustainable resource-efficient system. Goal 7 of the sustainable development goals of United Nation's 2030 Agenda [2] is directly promoting secure access to affordable, reliable, sustainable and modern energy for all. Within Europe, the European Green Deal, sets a strategy for no net emissions of greenhouse gases in 2050 and for decoupling resources from economic growth [3]. To assess policies in this context it is convenient to recognize the current situation and understand the dynamics in energy commodity prices and their co-movements at different long and medium-term frequencies.

The evolution of energy prices impact other non-energy primary commodities [4], exchange rates [5] and inflation [6], among others. Not only energy prices affect economic activity but are also influenced by it (as [7, 8] show for general commodity prices), being one of the main determinants of the real price of commodity shifts in the demand for commodities associated with unexpected fluctuations linked to the business cycle. This relation suggests that besides analyzing the long-run behaviour for policy issues, studying the cyclical frequency in energy prices is also of paramount importance. A second issue is related to decoupling among different energy prices as, on a theoretical and empirical basis, oil and natural gas are close substitutes in the long run. In this regard, some authors have found that oil prices drove US gas prices and that oil prices also led the co-movement between European and North American natural gas prices [9, 10]. Despite this evidence, US oil and gas prices seem to have decoupled since 2009 starting a new discussion on whether this is permanent [11, 12, 13]. Since target policies should be different if decoupling amongst markets occurs at the long run or at medium frequency, we tackle this problem addressing the particular frequencies at which markets might be decoupled.

To extract signals in a multivariate setup and understand their formation we introduce Multivariate Circular Singular Spectrum Analysis (M-CiSSA). Our proposal is an automated multivariate version of Singular Spectrum Analysis (SSA). SSA is a non-parametric procedure for signal extraction, see

for instance the survey by [14] or [15]. It is based on subspace algorithms and extracts the underlying signals of a time series like the long, medium or short-run cycles. SSA methodology chooses a window length L and builds a related trajectory matrix by putting together lagged pieces of the original time series and works with the Singular Value Decomposition of this matrix. The multivariate extension of this technique (M-SSA) [16] appears simultaneously with univariate SSA [17, 18]. M-SSA is able to extract patterns along time and amongst time series [19]. While originally only applied to climatology, since the work of [14] that compared different versions, the technique extended its application to a wide range of disciplines: Biometrics [20], image processing [21], geolocalization [22] and economic related problems [23, 24, 25, 26, 27, 28] amongst others. SSA and M-SSA are based on the singular value decomposition of different matrices of second order moments of a single or group of time series. Two alternatives are popular in the literature: Basic and Toeplitz SSA. However, both alternatives need to identify the frequencies associated to the estimated components after they have been extracted. To solve this problem in the univariate case, it is possible use an alternative circulant second order matrix that allows for closed formulae for eigenvalues and eigenvectors so as they can be linked to specific frequencies and, therefore, automate the procedure of assigning frequencies to the extracted principal components originating the so called Circulant SSA, CiSSA, [29].

The Multivariate Circulant Singular Spectrum Analysis, M-CiSSA, is a novel methodology that builds a multivariate trajectory matrix and performs a singular value decomposition by means of block circulant matrices whose singular values will identify the cross spectral density at different frequencies. This approach is going to have several advantages. First, eigenvalues and eigenvectors of each of these blocks will contain all the variability of the corresponding frequencies. This will allow to understand co-movements at different frequencies and even the cyclical position amongst the different variables. Second, we prove a theorem that states the reconstruction of the univariate components by the sum of the multivariate subcomponents. This is going to be very useful to further understand the formation of the individual cycles in terms of the multivariate common drivers.

The aim of this paper is to develop a new methodology, Multivariate Circulant SSA. We are able to extract signals associated to different frequencies understanding their formation in a multivariate setup. Therefore, this will help to understand co-movement and decoupling among a group of time series at specific frequencies. We apply it to jointly analyze the long and medium-run behaviour of energy commodity prices in order to: first, characterize the main cycles driving price fluctuations in the long and medium term; second, identify co-movements by frequency and clearly derive the differentiated behaviour of natural gas in US from the rest of energy commodities in the long and medium term; third, identify the additional decoupling of coals and natural gas in Japan only at the

medium-term cyclical frequency; and, fourth, discover which prices are held or sustained by forces outside the common evolution of the markets.

The paper is structured as follows. Section 2 presents M-CiSSA methodology. Section 3 the application to the understanding of the dynamics of 9 energy commodity real prices (oils, coals, natural gas and propane). Finally, section 4 concludes.

2 Methodology

SSA is a nonparametric technique in order to extract the underlying signals in a time series like the trend, cycle or seasonal component [15]. Different SSA variants, univariate and multivariate, are procedures in two stages: decomposition and reconstruction. In the first stage, decomposition, we transform the original vector of data into a related trajectory matrix and perform its singular value decomposition to obtain the so called elementary matrices. This corresponds to steps 1 and 2 in the algorithms. In the second stage, reconstruction, (steps 3 and 4 of the algorithms) we classify the elementary matrices into disjoint groups associating each group to the frequencies of an unobserved component (trend, cycle,...). Finally, every group is transformed into an unobserved component of the same size of the original time series by diagonal averaging.

Before describing our new proposed methodology, M-CiSSA, we will briefly describe the univariate algorithm and give some preliminary results that we need in order to show how to diagonalize the circulant matrix of second moments that we use in our procedure.

2.1 Univariate SSA

Let $\{x_t\}$ be a stochastic process $t \in \mathcal{T}$ whose realization of length T is given by $\mathbf{x} = (x_1, ..., x_T)'$[1], where the prime denotes transpose and let L be a positive integer, called the window length, such that $1 < L < T/2$. The 4 steps of the algorithm are as follows:

1st step: Embedding

We build an $L \times N$ trajectory matrix $\mathbf{X}$, $N = T - L + 1$, as

$$\mathbf{X} = (\mathbf{x}_1|...|\mathbf{x}_N) = \begin{pmatrix} x_1 & x_2 & x_3 & ... & x_N \\ x_2 & x_3 & x_4 & ... & x_{N+1} \\ \vdots & \vdots & \vdots & \vdots & \vdots \\ x_L & x_{L+1} & x_{L+2} & ... & x_T \end{pmatrix}. \tag{1}$$

[1]For simplicity, we use the same notation for the stochastic process and for the observed time series. It will be clear from the context if we are referring to the population or to the sample. If it were not, we would explicitly clarify it in the main text.

2nd step: Decomposition

In the second step, we perform the singular value decomposition (SVD) of the trajectory matrix $\mathbf{X} = \mathbf{U}\mathbf{D}^{1/2}\mathbf{V}'$ where $\mathbf{U}$ is the $L \times L$ matrix whose columns $\mathbf{u}_k$ are the $L \times 1$ eigenvectors of the second moment matrix $\mathbf{S} = \mathbf{X}\mathbf{X}'$, $\mathbf{D} = \text{diag}(\tau_1, ..., \tau_L)$, $\tau_1 \geq ... \geq \tau_L \geq 0$, are the eigenvalues of $\mathbf{S}$ and $\mathbf{V}$ is the $N \times L$ matrix whose L columns $\mathbf{v}_k$ are the $N \times 1$ eigenvectors of $\mathbf{X}'\mathbf{X}$ associated to nonzero eigenvalues. In this step we decompose the trajectory matrix $\mathbf{X}$ as the sum of the elementary matrices $\mathbf{X}_k$ of rank 1,

$$\mathbf{X} = \sum_{k=1}^{r} \mathbf{X}_k = \sum_{k=1}^{r} \mathbf{u}_k \mathbf{w}_k',$$

where $\mathbf{w}_k = \mathbf{X}'\mathbf{u}_k = \sqrt{\tau_k}\mathbf{v}_k$, being $\sqrt{\tau_k}$ the singular values of the $\mathbf{X}$ matrix, and $r = \max_{\tau_k > 0} \{k\} = \text{rank}\,(\mathbf{X})$.

3rd step: Grouping

The third step groups the elementary matrices $\mathbf{X}_k$ into G disjoint sets according to the relevant information associated with a specific group of frequencies. To do so we sum up the elementary matrices within each group. Let $I_j, j = 1, ..., G$ be each disjoint group of indexes associated to the corresponding eigenvectors. The matrix $\mathbf{X}_{I_j} = \sum_{k \in I_j} \mathbf{X}_k$ is associated to the I_j group. The decomposition of the trajectory matrix into these groups is given by $\mathbf{X} = \mathbf{X}_{I_1} + ... + \mathbf{X}_{I_G}$.

4th step: Reconstruction

Finally, we transform the matrices from the previous step $\mathbf{X}_{I_j} = (\widetilde{x}_{ij})$ into time series of size T, $\widetilde{\mathbf{x}}^{(j)} = (\widetilde{x}_1^{(j)}, ..., \widetilde{x}_T^{(j)})'$, by diagonal averaging. This means to average the elements of $\mathbf{X}_{I_j}$ over its antidiagonals.

Notice that to perform the Singular Value Decomposition of the trajectory matrix is equivalent to diagonalize the second ordern matrix $\mathbf{X}'\mathbf{X}$. The procedure CiSSA substitutes the second order matrix $\mathbf{X}'\mathbf{X}$ by a circulant counterpart [29]. The advantages of the latest are twofold: first, they have known expression for their eigenvalues and eigenvectors and, second, these are related to specific frequencies and, therefore, can be used to extract signals associated to any desired frequency specified beforehand.

2.2 Preliminary results

M-CiSSA is a multivariate version of SSA based on block circulant matrices applied to a group of a zero mean time series, instead of to a single one. Let $\mathbf{x}_t = \left(x_t^{(1)}, \cdots, x_t^{(M)}\right)'$ be the vector of time series at time t with second moments given by $\mathbf{\Gamma}_k = E[\mathbf{x}_{t+k}\mathbf{x}_t'], k = 0, \pm 1, \cdots, \pm\,(L-1)$.

Before introducing our proposed generalization, we need to define the big trajectory matrix associated to our set of time series and study its second moment properties.

We build a big trajectory matrix where we expand every scalar element x_t in (1) by its vector

counterpart $\mathbf{x}_t = \left(x_t^{(1)}, \cdots, x_t^{(M)}\right)'$. Therefore, the big trajectory matrix, of dimensions $LM \times N$, is

$$\mathbf{X} = \begin{pmatrix} \mathbf{x}_1 & \mathbf{x}_2 & \cdots & \mathbf{x}_N \\ \mathbf{x}_2 & \mathbf{x}_3 & \cdots & \mathbf{x}_{N+1} \\ \vdots & \vdots & \vdots & \vdots \\ \mathbf{x}_L & \mathbf{x}_{L+1} & \cdots & \mathbf{x}_T \end{pmatrix} = \begin{pmatrix} x_1^{(1)} & x_2^{(1)} & \cdots & x_N^{(1)} \\ \vdots & \vdots & \vdots & \vdots \\ x_1^{(M)} & x_2^{(M)} & \cdots & x_N^{(M)} \\ x_2^{(1)} & x_3^{(1)} & \cdots & x_{N+1}^{(1)} \\ \vdots & \vdots & \vdots & \vdots \\ x_2^{(M)} & x_3^{(M)} & \cdots & x_{N+1}^{(M)} \\ \vdots & \vdots & \vdots & \vdots \\ x_L^{(1)} & x_{L+1}^{(1)} & \cdots & x_T^{(1)} \\ \vdots & \vdots & \vdots & \vdots \\ x_L^{(M)} & x_{L+1}^{(M)} & \cdots & x_T^{(M)}. \end{pmatrix} \tag{2}$$

Consider the sequence of lagged cross variance-covariance matrices of the population as a function of the window length L. Each matrix in that sequence is an $L \times L$ block Toeplitz matrix with $M \times M$ blocks resulting in a $LM \times LM$ Hermitian matrix. Let

$$\mathbf{T}_L = \left[\mathbf{\Gamma}_{ij} = \mathbf{\Gamma}_{i-j}; i, j = 1, \cdots, L\right]. \tag{3}$$

It is well known that the sequence $\{\mathbf{\Gamma}_k\}_{k\in\mathbb{Z}}$ can be generated as

$$\mathbf{\Gamma}_k = \int_0^1 \mathbf{F}(\omega) \exp(-i2\pi k\omega) d\omega, \ \forall k \in \mathbb{Z}$$

where $\omega \in [0, 1]$ is the frequency in cycles per unit of time and $\mathbf{F}(\omega)$ is the spectral density matrix of the stochastic process of the vector time series $\mathbf{x}_t$, that is the "matrix" Fourier series given by

$$\mathbf{F}(\omega) = \sum_{k=-\infty}^{\infty} \mathbf{\Gamma}_k \exp(i2\pi k\omega), \ \omega \in [0, 1]. \tag{4}$$

The sequence $\{\mathbf{\Gamma}_k\}_{k\in\mathbb{Z}}$ are the Fourier coefficients of the matrix-valued function $\mathbf{F}(\omega)$. As a consequence, the continuous and 2π-periodic matrix-valued function $\mathbf{F}(\omega)$ of real variable is the generating function or symbol of the matrix $\mathbf{T}_L(\mathbf{F}) = \mathbf{T}_L$ that originates the sequence of block Toeplitz matrices that we denote $\{\mathbf{T}_L(\mathbf{F})\}$.

With this approach we do not have a closed formula for the eigenvalues and eigenvectors of the Toeplitz matrix of second moments given in (3). This problem could be solved if instead of block Toeplitz matrices we use block circulant matrices.

Let $\mathbf{C}_L$ be an $L \times L$ block circulant matrix with blocks $M \times M$, that is, $\mathbf{C}_L$ is an $LM \times LM$ matrix of the form

$$\mathbf{C}_L = \begin{pmatrix} \mathbf{\Omega}_0 & \mathbf{\Omega}_1 & \mathbf{\Omega}_2 & \cdots & \mathbf{\Omega}_{L-1} \\ \mathbf{\Omega}_{L-1} & \mathbf{\Omega}_0 & \mathbf{\Omega}_1 & \ddots & \vdots \\ \mathbf{\Omega}_{L-2} & \mathbf{\Omega}_{L-1} & \mathbf{\Omega}_0 & \ddots & \mathbf{\Omega}_2 \\ \vdots & \ddots & \ddots & \ddots & \mathbf{\Omega}_1 \\ \mathbf{\Omega}_1 & \cdots & \mathbf{\Omega}_{L-2} & \mathbf{\Omega}_{L-1} & \mathbf{\Omega}_0 \end{pmatrix} \tag{5}$$

where $\mathbf{\Omega}_k \in \mathbb{C}^{M \times M},\ k = 0, 1, \cdots, L-1$. We say that $\mathbf{C}_L$ is block circulant since each block row is built from a right shift of the blocks of the previous block row. Each block of $\mathbf{C}_L$ can be generated [30] as

$$\mathbf{\Omega}_k = \frac{1}{L} \sum_{j=0}^{L-1} \mathbf{F}\left(\frac{j}{L}\right) \exp\left(\frac{i2\pi jk}{L}\right),\ k = 0, \cdots, L-1$$

being $\mathbf{F}(\omega)$ the generating function of the sequence $\{\mathbf{T}_L(\mathbf{F})\}$ which is also the symbol of the matrix $\mathbf{C}_L(\mathbf{F}) = \mathbf{C}_L$ and generates the sequence of block circulant matrices $\{\mathbf{C}_L(\mathbf{F})\}$. Moreover, the two block matrices sequences $\{\mathbf{T}_L(\mathbf{F})\}$ and $\{\mathbf{C}_L(\mathbf{F})\}$ are asymptotically equivalent as $L \to \infty$, $\mathbf{T}_L(\mathbf{F}) \sim \mathbf{C}_L(\mathbf{F})$, in the sense that both matrices have bounded eigenvalues and $\lim_{L\to\infty} \frac{\|\mathbf{T}_L(\mathbf{F}) - \mathbf{C}_L(\mathbf{F})\|_F}{\sqrt{L}} = 0$ [30, Lemma 6.1], where $\|\cdot\|_F$ is the Frobenius norm.

The advantage of using the block circulant matrix $\mathbf{C}_L$ instead of the block Toeplitz matrix $\mathbf{T}_L$ is that the former can be block diagonalized (in fact we will fully diagnolize it, not only by blocks), while the later is not. However, in order to build the block matrix (5), we should either know the matrix function $\mathbf{F}$ or the infinite sequence $\{\mathbf{\Gamma}_k\}_{k\in\mathbb{Z}}$. We realize that, in practice, we will have a finite number of second order matrices so, in order to make this approach operational we generalize the results given in [31] for the continuous and 2π-periodic scalar function f to the continuous and 2π-periodic matrix function $\mathbf{F}$. In particular, similarly to what is proposed in [31] for 1×1 blocks, we suggest to use as $M \times M$ blocks of the first row in $\mathbf{C}_L$:

$$\widetilde{\mathbf{\Omega}}_k = \frac{k}{L}\mathbf{\Gamma}_{L-k} + \frac{L-k}{L}\mathbf{\Gamma}_{-k},\ k = 0, \cdots, L-1. \tag{6}$$

This way of defining the block circulant matrix $\mathbf{C}_L$ is associated with the continuous and 2π-periodic matrix function $\widetilde{\mathbf{F}}$,

$$\widetilde{\mathbf{F}}(\omega) = \frac{1}{L} \sum_{m=1}^{L} \sum_{l=1}^{L} \mathbf{\Gamma}_{l-m} \exp\left(i2\pi\left(l-m\right)\omega\right),\ \omega \in [0,1], \tag{7}$$

that generates the sequence of block circulant matrices $\left\{\mathbf{C}_L\left(\widetilde{\mathbf{F}}\right)\right\}$. Theorem 1 shows the asymptotic

equivalence between the sequences $\{\mathbf{T}_L(\mathbf{F})\}$ and $\left\{\mathbf{C}_L\left(\widetilde{\mathbf{F}}\right)\right\}$, denoted as $\mathbf{T}_L(\mathbf{F}) \sim \mathbf{C}_L(\widetilde{\mathbf{F}})$. This theorem is the basis of our proposed algorithm since we will use the later sequences in our Multivariate Circulant SSA proposal, that we label as M-CiSSA.

Theorem 1 *Let $\mathbf{F} : [0,1] \to \mathbb{C}^{M\times N}$ be a matrix-valued function of real variable which is continuous and 2π-periodic and let $\widetilde{\mathbf{F}}$ be the matrix-valued function defined in (7) from the Fourier coefficients of the matrix-valued function $\mathbf{F}$, then, $\mathbf{T}_L(\mathbf{F}) \sim \mathbf{C}_L\left(\widetilde{\mathbf{F}}\right)$.*

Proof. The proof is given in the appendix. ■

Finally, we end up this preliminary section with auxiliary results that we need before proposing our algorithm showing how the block circulant matrix sequence $\{\mathbf{C}_L(\mathbf{F})\}$ is diagonalized. For any matrix valued function $\mathbf{F} : [0,1] \to \mathbb{C}^{M\times M}$ which is continuos and 2π-periodic, the block circulant matrix $\mathbf{C}_L(\mathbf{F})$ is characterized by a block diagonalization given by

$$\mathbf{C}_L(\mathbf{F}) = (\mathbf{U}_L \otimes \mathbf{I}_M)\,\mathrm{diag}(\mathbf{F}_1, \cdots, \mathbf{F}_L)\,(\mathbf{U}_L \otimes \mathbf{I}_M)^* \tag{8}$$

where $\mathbf{U}_L$ is the Fourier unitary matrix given by

$$\mathbf{U}_L = L^{\frac{1}{2}}\left[\exp\left(\frac{-i2\pi(j-1)(k-1)}{L}\right);\ j,k = 1,\cdots,L\right]$$

and $\mathbf{I}_M$ is the identity matrix of order M. Each block $\mathbf{F}_k = \mathbf{F}\left(\frac{k-1}{L}\right)$, $k = 1,\cdots,L$ represents the cross spectral density matrix of the multivariate stochastic process $\mathbf{x}_t$ for the frequency $\omega_k = \frac{k-1}{L}, k = 1,\cdots,L$ and can be unitarily diagonalized. In this way, we obtain that $\mathbf{F}_k = \mathbf{E}_k\mathbf{D}_k\mathbf{E}_k^*$ with $\mathbf{E}_k \in \mathbb{C}^{M\times M}$ and $\mathbf{E}_k\mathbf{E}_k^* = \mathbf{E}_k^*\mathbf{E}_k = \mathbf{I}_M$, where $\mathbf{E}_k = [\mathbf{e}_{k,1}|\cdots|\mathbf{e}_{k,M}]$ contains the eigenvectors and the diagonal matrix $\mathbf{D}_k = \mathrm{diag}(\lambda_{k,1},\cdots,\lambda_{k,M})$ contains the ordered eigenvalues $\lambda_{k,1} \geq \cdots \geq \lambda_{k,M} \geq 0$ of $\mathbf{F}_k$. Therefore, the unitary diagonalization of the Hermitian matrix $\mathbf{C}_L(\mathbf{F})$ is given by $\mathbf{C}_L(\mathbf{F}) = \mathbf{VDV}^*$ with

$$\mathbf{V} = (\mathbf{U}_L \otimes \mathbf{I}_M)\,\mathbf{E} \in \mathbb{C}^{LM\times LM} \tag{9}$$

where $\mathbf{E} = \mathrm{diag}(\mathbf{E}_1,\cdots,\mathbf{E}_L)$ and $\mathbf{D} = \mathrm{diag}(\mathbf{D}_1,\cdots,\mathbf{D}_L)$. As a consequence, there are M eigenvectors associated to each frequency $\omega_k = \frac{k-1}{L}$. The *j-th* eigenvector $\mathbf{v}_j$, $j = 1,...,LM$ of the matrix $\mathbf{C}_L(\mathbf{F})$ is given by

$$\mathbf{v}_j = \mathbf{v}_{(k-1)M+m} = \mathbf{v}_{k,m} = \mathbf{u}_k \otimes \mathbf{e}_{k,m}$$

for $k = 1,\cdots,L$ and $m = 1,\cdots,M$ where $\mathbf{u}_k$ is the *k-th* column of the Fourier unitary matrix $\mathbf{U}_L$ and

$\mathbf{e}_{k,m}$ is the *m-th* eigenvector of the cross spectral density matrix $\mathbf{F}_k$. Notice that $\mathbf{F}$ is symmetric with respect to the frequency $\frac{1}{2}$ as deduced from (4). This means $\mathbf{F}_k = \mathbf{F}_{L+2-k}^T;\ k = 2, \cdots, \lfloor \frac{L+1}{2} \rfloor$. So the corresponding eigenvectors are conjugated $\mathbf{E}_k = \overline{\mathbf{E}}_{L+2-k}$ and the associated eigenvalues are equal $\mathbf{D}_k = \mathbf{D}_{L+2-k}$. Proposition 2 states how to orthogonally diagonalize the circulant matrix $\mathbf{C}_L(\mathbf{F})$.

Proposition 2 *Let $\mathbf{C}_L(\mathbf{F})$ the block circulant matrix given by (8) and let $\mathbf{V}$ the unitary matrix obtained by (9) that unitarily diagonalizes $\mathbf{C}_L(\mathbf{F})$. The set of vectors $\{\widetilde{\mathbf{v}}_{k,m}\}_{k,m=1}^{L,M}$ defined $\forall\, m = 1, \cdots, M$ by*

$$\tilde{\mathbf{v}}_{k,m} = \begin{cases} \mathbf{v}_{k,m} & k = 1 \text{ and } \frac{L}{2}+1 \text{ if } L \text{ is even} \\ \sqrt{2}\mathcal{R}_{\mathbf{v}_{k,m}} & k = 2, \cdots, \lfloor \frac{L+1}{2} \rfloor \\ \sqrt{2}\mathcal{R}_{\mathbf{v}_{L+2-k,m}} & k = \lfloor \frac{L+1}{2} \rfloor + 1, \cdots, L \end{cases}$$

is an orthonormal basis of $\mathbb{R}^{LM}$ that orthogonally diagonalizes the matrix $\mathbf{C}_L(\mathbf{F})$, $\mathbf{C}_L(\mathbf{F}) = \widetilde{\mathbf{V}}\mathbf{D}\widetilde{\mathbf{V}}'$, where $\mathcal{R}_{\mathbf{v}}$ and $\mathcal{I}_{\mathbf{v}}$ are the real and imaginary parts of the vector $\mathbf{v}$ and $\widetilde{\mathbf{V}} = [\widetilde{\mathbf{v}}_1 | \cdots | \widetilde{\mathbf{v}}_{LM}]$ being $\widetilde{\mathbf{v}}_j = \widetilde{\mathbf{v}}_{k,m}$ with $j = (k-1)M + m \quad \forall\, k = 1, \cdots, L$ and $m = 1, \cdots, M$.

Proof. The proof is given in the appendix. ■

After all these preliminary results, we are able to introduce our proposed procedure for multivariate signal extraction based on block circulant matrices of second moments.

2.3 Multivariate Circulant SSA

Let $\mathbf{x}_t = \left(x_t^{(1)}, \cdots, x_t^{(M)}\right)'$, be an M-dimensional stationary and, for simplicity, zero mean real time series of length T, and let L, the so called window length, be an integer such that $1 < L \leq \frac{T}{2}$ with $N = T - L + 1$. The M-CiSSA algorithm follows the following four steps:

1st step: Embedding

Form the big trajectory matrix $\mathbf{X}$ as in (2).

2nd step: Decomposition

In this step we make the spectral decomposition of the trajectory matrix from the first step by orthogonally diagonalizing the block circulant matrix $\mathbf{S_C}$ given by

$$\mathbf{S_C} = \begin{pmatrix} \hat{\mathbf{\Omega}}_0 & \hat{\mathbf{\Omega}}_1 & \cdots & \hat{\mathbf{\Omega}}_{L-1} \\ \hat{\mathbf{\Omega}}_{L-1} & \hat{\mathbf{\Omega}}_0 & \ddots & \vdots \\ \vdots & \ddots & \ddots & \hat{\mathbf{\Omega}}_1 \\ \hat{\mathbf{\Omega}}_1 & \cdots & \hat{\mathbf{\Omega}}_{L-1} & \hat{\mathbf{\Omega}}_0 \end{pmatrix}$$

where $\hat{\mathbf{\Omega}}_k$, $k = 1, ..., L-1$ is constructed as in (6) considering sample estimates of the lagged autoco-

variances matrices $\hat{\mathbf{\Gamma}}_k$. Making use of the same reasoning as before, notice that by construction $\mathbf{S_C}$ is asymptotically equivalent to the block Toeplitz matrix $\mathbf{S_T}$

$$\mathbf{S_T} = \begin{pmatrix} \hat{\mathbf{\Gamma}}_0 & \hat{\mathbf{\Gamma}}_{-1} & \cdots & \hat{\mathbf{\Gamma}}_{1-L} \\ \hat{\mathbf{\Gamma}}_1 & \hat{\mathbf{\Gamma}}_0 & \ddots & \vdots \\ \vdots & \ddots & \ddots & \hat{\mathbf{\Gamma}}_{-1} \\ \hat{\mathbf{\Gamma}}_{L+1} & \cdots & \hat{\mathbf{\Gamma}}_1 & \hat{\mathbf{\Gamma}}_0 \end{pmatrix}.$$

Given the results in the previous sub-section, the unitary diagonalization of $\mathbf{S_C}$ is given by

$$\mathbf{S_C} = (\mathbf{U}_L \otimes \mathbf{I}_M)\, \hat{\mathbf{E}}\hat{\mathbf{D}}\hat{\mathbf{E}}^* \,(\mathbf{U}_L \otimes \mathbf{I}_M)^* = \hat{\mathbf{V}}\hat{\mathbf{D}}\hat{\mathbf{V}}^*$$

where $\hat{\mathbf{E}}$, $\hat{\mathbf{D}}$ and $\hat{\mathbf{V}}$ are the sample counterparts of the matrices previously used. Finally, the orthogonal diagonalization of $\mathbf{S_C}$ is given by $\mathbf{S_C} = \widetilde{\mathbf{V}}\hat{\mathbf{D}}\widetilde{\mathbf{V}}'$ where the orthonormal matrix $\widetilde{\mathbf{V}} = [\widetilde{\mathbf{v}}_1|\cdots|\widetilde{\mathbf{v}}_{LM}] \in \mathbb{R}^{LM\times LM}$ is constructed as in Proposition 2.

For each frequency $\omega_k = \frac{k-1}{L},\ k = 1, \cdots, L$, there are M associated eigenvectors. Therefore, the *m-th* elementary matrix associated to ω_k is given by

$$\mathbf{X}_{k,m} = \widetilde{\mathbf{v}}_{k,m}\mathbf{w}'_{k,m} = \widetilde{\mathbf{v}}_{k,m}\widetilde{\mathbf{v}}'_{k,m}\mathbf{X} \in \mathbb{R}^{LM\times N}.$$

The elements of the eigenvector $\widetilde{\mathbf{v}}_{k,m}$ corresponding to the *i-th* time series are collected in $\widetilde{\mathbf{v}}^{(i)}_{k,m}$ by

$$\widetilde{\mathbf{v}}^{(i)}_{k,m} = \left(\mathbf{I}_L \otimes \mathbf{1}'_{M,i}\right)\widetilde{\mathbf{v}}_{k,m} \tag{10}$$

where $\mathbf{1}_{M,i}$ is a column vector of length M with a 1 in the *i-th* position and 0 in the remaining places. Therefore, the elementary matrix for the *m-th* subcomponent at frequency ω_k for the *i-th* series is obtained as

$$\mathbf{X}^{(i)}_{k,m} = \widetilde{\mathbf{v}}^{(i)}_{k,m}\mathbf{w}'_{k,m} = \widetilde{\mathbf{v}}^{(i)}_{k,m}\widetilde{\mathbf{v}}'_{k,m}\mathbf{X} \in \mathbb{R}^{L\times N}. \tag{11}$$

As a consequence, the trajectory matrix can be decomposed as

$$\mathbf{X} = \sum_{k,m}\mathbf{X}_{k,m} = \sum_{k,m}\mathbf{P}\begin{pmatrix} \mathbf{X}^{(1)}_{k,m} \\ \vdots \\ \mathbf{X}^{(M)}_{k,m} \end{pmatrix} \tag{12}$$

where $\mathbf{P}$ is a permutation matrix built for this purpose.

The contribution of the elementary matrix $\mathbf{X}_{k,m}$ given by (12) is the ratio $\frac{\hat{\lambda}_{k,m}}{\sum_{k,m}\hat{\lambda}_{k,m}}$. Also considering (10) the participation index [32] of the *i-th* time series within the *m-th* subcomponent at frequency ω_k is defined as

$$\pi_{k,m}^{(i)} = \hat{\lambda}_{k,m}\left(\widetilde{\mathbf{v}}_{k,m}^{(i)}\right)'\widetilde{\mathbf{v}}_{k,m}^{(i)}\,. \tag{13}$$

3rd step: Grouping

The spectral density function of the vector process $\mathbf{x}_t$ is symmetric and therefore $\hat{\mathbf{F}}_k = \hat{\mathbf{F}}'_{L+2-k}$ for $k = 2, \cdots, G$, where $G = \left\lfloor \frac{L+1}{2} \right\rfloor$. Then $\hat{\mathbf{D}}_k = \hat{\mathbf{D}}_{L+2-k}$ and $\hat{\mathbf{E}}_k = \bar{\hat{\mathbf{E}}}_{L+2-k}$ and, consequently, the subcomponents $\mathbf{w}_{k,m} = \mathbf{X}'\widetilde{\mathbf{v}}_{k,m}$ and $\mathbf{w}_{L+2-k,m} = \mathbf{X}'\widetilde{\mathbf{v}}_{L+2-k,m}$ are harmonics of the same frequency. This motivates the creation of elementary pairs per subcomponent and frequency $B_{k,m} = \{(k,m),(L+2-k,m)\}$ for $k = 2, \cdots, G$ except $B_{1,m} = \{(1,m)\}$ and occasionally $B_{\frac{L}{2}+1,m} = \left\{\left(\frac{L}{2}+1, m\right)\right\}$ if L is even. The matrices corresponding to the pairs $B_{k,m}$ are given by the sum of two elementary matrices per subcomponent and frequency

$$\mathbf{X}_{B_{k,m}} = \mathbf{X}_{k,m} + \mathbf{X}_{L+2-k,m}. \tag{14}$$

Therefore, both the associated matrices to the elementary pairs $B_{k,m}$ by subcomponent and frequency and the oscillatory components obtained from them are previously identified with a determined frequency as in the univariate case.

Under the assumption of separability proven by [29] we define D disjoint groups of the elementary pairs per subcomponent and frequency. The resulting matrix for each of the disjoint groups is defined as the sum of the associated matrices to the pairs $B_{k,m}$ included. If $I_j = \left\{B_{k_{j_1},m_{j_1}}, ..., B_{k_{jq},m_{jq}}\right\}$, $j = 1, ..., D$ is each disjoint group of j_q pairs $B_{k,m}$ with $1 \leq j_q \leq GM$, then the matrix $\mathbf{X}_{I_j}$ from group I_j is calculated as the sum of the corresponding matrices defined by (14), $\mathbf{X}_{I_j} = \sum_{B_{k,m}\in I_j}\mathbf{X}_{B_{k,m}}$. Therefore, the decomposition of the trajectory matrix $\mathbf{X}$ given by (12) produces the expansion

$$\mathbf{X} = \mathbf{X}_{I_1} + \mathbf{X}_{I_2} + \cdots + \mathbf{X}_{I_D}.$$

If we wish to extract the oscillatory component of periodicity $\frac{L}{k-1}$, the appropriate group is $B_k = \{B_{k,m}\ \forall\, m, 1 \leq m \leq M\}$ being the resulting matrix $\mathbf{X}_{B_k} = \sum_{m=1}^{M}\mathbf{X}_{B_{k,m}}$

4th step: Reconstruction

Finally, each $L \times N$ matrix $\mathbf{X}_{I_j}$ of vectors $M \times 1$ of the previous step is transformed into a new time series of length T by diagonal averaging producing the reconstructed time series $\widetilde{\mathbf{x}}_{I_j,t} = \left(\widetilde{x}_{I_j,t}^{(1)}, \cdots, \widetilde{x}_{I_j,t}^{(M)}\right)'$. If $\mathbf{x}_{r,s}^{I_j}$ are the vector elements of the matrix $\mathbf{X}_{I_j}$, then the values of the recon-

structed vector time series $\widetilde{\mathbf{x}}_{I_j,t}$, with $L < N$ are calculated as in [33] but the formula is adapted to vectors to "hankelize" the matrix $\mathbf{X}_{I_j}$:

$$\tilde{\mathbf{x}}_{I_j,t} = \begin{cases} \frac{1}{t}\sum_{i=1}^{t} \mathbf{x}_{i,t-i+1}^{I_j} & 1 \leq t < L \\ \frac{1}{L}\sum_{i=1}^{L} \mathbf{x}_{i,t-i+1}^{I_j} & L \leq t \leq N \\ \frac{1}{T-t+1}\sum_{i=t-T+L}^{L} \mathbf{x}_{i,t-i+1}^{I_j} & N < t \leq T \end{cases}$$

The reconstructed multivariate times series resulting from $B_{k,m}$ are called elementary reconstructed vector time series by subcomponent m and frequency k.

By the separability property, it holds that the reconstruction preserves the information, that is, the analyzed time series $\mathbf{x}_t$ can be decomposed as the sum of D vector time series obtained in the previous step as follows $\mathbf{x}_t = \sum_{j=1}^{D} \widetilde{\mathbf{x}}_{I_j,t}$.

The M-CiSSA algorithm described so far requires stationary time series. However, it is straightforward to show that it can also be applied to nonstationary time series. Other versions of multivariate SSA, Basic SSA [16] and Toeplitz SSA [19], are also implemented on nonstationary time series. In the case of Circulant SSA, its validity is shown for nonstationary univariate time series aproximating the discontinuities of the spectrum by a pseudo-spectrum [29]. The same approximation can be applied in the case of M series instead of just one. More recently, there are examples of applying alternative versions of SSA to nonstationary multivariate time series [25, 34, 35]. In a related but different context, principal components and lagged principal components are also used over nonstationary time series [36].

2.4 Uniqueness between CiSSA and M-CiSSA

The univariate estimation in CiSSA of the oscillatory component of the *i-th* series for each frequency $\omega_k = \frac{k-1}{L}$, $k = 1, \cdots, L$, originates a single time series or component associated to the elementary matrix by frequency $\mathbf{X}_k^{(i)}$. However, the estimation of that same oscillatory component by M-CiSSA produces M series or subcomponents respectively associated to the M elementary matrices by subcomponent and frequency $\mathbf{X}_{k,m}^{(i)}$. The sum of these matrices, $\sum_{m=1}^{M} \mathbf{X}_{k,m}^{(i)}$, originates the estimation in M-CiSSA of the oscillatory component of the *i-th* series at frequency ω_k. Theorem 3 proves the identity.

Theorem 3 *The oscillatory compoments derived from the matrices* $\mathbf{X}_k^{(i)}$ *and* $\sum_{m=1}^{M} \mathbf{X}_{k,m}^{(i)}$ *of any i-th time series at each frequency* ω_k *obtained with univariate and multivariate CiSSA, respectivelly, are identical. That is, the oscillatory component of any i-th time series for each frequency* ω_k *is unique.*

Proof. The proof is given in the appendix. ■

This result allows to use M-CiSSA as a way to de-noise the extracted signals and also to extract the common spectral signals and estimate co-movements. Regarding de-noising, M-CiSSA allows to separate the signal from an over imposed colored noise, as defined by [37], by selecting a reduced number of components associated to the non-null eigenvalues estimated for the frequency ω_k. In general, to estimate the signal of an harmonic it will be enough to select a small number of subcomponents associated to their higher eigenvalues that will characterize both the amplitude and the dating of the oscillatory components. In this sense, the subcomponents help to extract the common spectral signals as well as the co-movements in order to analyze their characterization (procyclical or anticyclical) and cyclical position (leading, coincident or lagging) of the oscillatory components [34]. Therefore, these subcomponents describe the formation of the oscillatory components in a multivariate setup.

Theorem 3 also proves the empirical result by [19] that, in M-SSA, an oscillatory pair does not explain all the variability due to an harmonic. Classical versions of M-SSA only consider the highest eigenvalues and omit information related to that harmonic. This information may have a great interest for economic analysis because it allows to observe, for each of the series, the different gaps for the same oscillatory component.

Another advantage of M-CiSSA with respect to the other M-SSA approaches is that gaps for each frequency are known beforehand and this avoids to make a search across all LM subcomponents.

3 Application

We apply M-CiSSA to the multivariate analysis of the monthly Primary Commodity Energy Prices (ENERGY) published by the IMF from January 1992 until February 2020 (338 observations). ENERGY comprises a set of nine commodity prices: Australian and South African Coal (COALAU, COALSA); Brent, Dubai and Wext Texas Intermediate Crude Oil (OILBRE, OILDUB, OILWTI); European, Indonesian and US Natural Gas (NGASEU, NGASJP, NGASUS) and Propane (PROPANE). Original prices in US$ have been deflated by the US Consumer Price Index to turn them into real terms [2] and have been transformed into index numbers (2016=100) for homogeneity. The choice of the deflator will not affect our results, it has little impact on the analysis of long-term price trends and it would presumably be a much more important issue in the short-run fluctuations [38]. Figure 1 shows the graphs of these nine commodities.

Before applying CiSSA and M-CiSSA we only need to choose one parameter, that is, the window

[2]The consideration of the data directly in nominal terms show the same conclusions. Results are available upon request.

Figure 1. Primary Energy Commodity Prices (Real terms based on IMF data, index 2006=100).

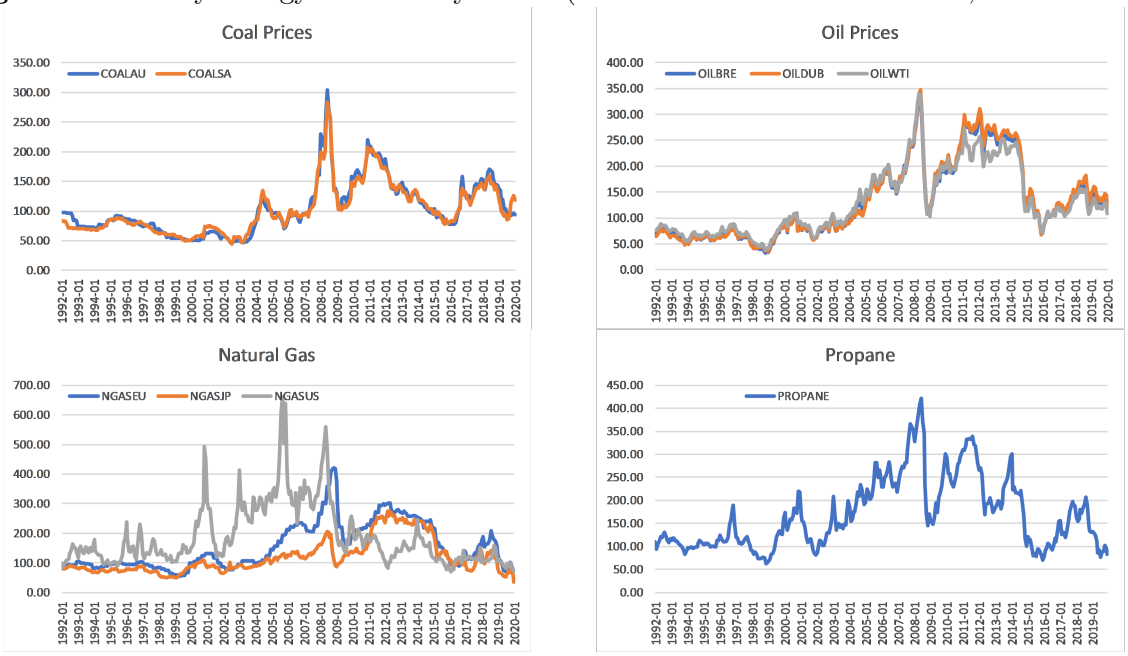

k	1	2	3	4	5	6	9
Period	inf	96	48	32	24	19	12
Contribution	52.8	20.3	7.5	6.7	2.9	2.2	0.7

Table 1. Accumulated contribution of each frequency over total variability.

length L. Due to the monthly periodicity, the first consideration is that L should be multiple of 12. On the other hand, L must also be multiple of the cycle periods to be analyzed [15]. Given the number of observations, $T = 338$, and the classification of cycles within primary commodity prices literature into medium (8 to 20 years) and super cycles (between 20 and 70 years) according to their duration, we are aware that we cannot study super cycles, but we can try to analyze at least periodicities up to 8 years as in the first group of cycles. Also see that 8 years is usually considered as the maximum in business cycle related literature for macroeconomic time series. Therefore, we choose $L = 96$ and build the trajectory matrix and the associated block circulant matrix made of 96 blocks of size 9×9. Each block is associated to a frequency as $w_k = \frac{k-1}{L}$ and within each block we can further diagonalize and understand its formation.

Table 1 shows the accumulated contribution of each frequency, defined as the trace of the corresponding block over the total matrix. This information allows to identify the main fluctuations that drive this group of series. The accumulated contribution shows that the trend is the most informative capturing 52.8% of the total variability. Also cycles of periodicity 96 months (8 years) are explaining

k	Period	Subcomponents		
		1	2	3
1	inf	80.1	99.3	99.7
2	96	68.3	94.8	98.5

Table 2. Accumulated contribution of the subcomponents over the variability of each frequency.

Eigenvector	COALAU	COALSA	OILBRE	OILDUB	OILWTI	NGASEU	NGASJP	NGASUS	PROPANE
Trend									
1	4.4	4.1	17.0	18.7	13.6	18.1	7.9	3.1	12.9
2	2.1	1.4	1.5	2.3	0.1	0.2	3.5	82.6	6.5
Cycle									
1	2.4	2.1	15.5	16.6	11.9	17.9	10.0	8.1	15.6
2	7.7	5.0	3.2	3.6	0.5	0.5	10.4	67.9	1.2
3	23.9	17.1	0.1	0.4	0.5	10.8	27.4	11.5	8.3

Table 3. Relative weights of the main eigenvectors for the trend and the 8-year cycle.

20.3% of the total variability. Therefore, by analyzing trend and 8-year cycles we are explaining almost 75% of the variability of energy primary commodity prices.

3.1 Long-run behaviour

The information about the trend is represented by the first 9×9 block of the approximation to the cross spectral density. Therefore, the eigenstructure of this first block matrix contains the information regarding the variability in the long run. Within the 52.8% variability corresponding to the trend, Table 2 shows that this is mainly explained by the two first eigenvalues, as they account for 80.1% and 19.2% respectively summing up a total of 99.3% with only these two subcomponents. Therefore, understanding the fluctuations implied these two eigenvectors will characterize the long-run drivers of these 9 series. From equation (9), the eigenvectors corresponding to the block $k = 1$ are just vectors of ones multiplied by a constant according to the relative weights of each series in the eigenvector and they are capturing the changing level of the series. Table 3 shows the relative weight of each variable in the first and second eigenvectors. Notice that the first eigenvector is a weighted average of all the series with a small contribution of NGASUS that becomes the main driver in the second eigenvector. So, our first conclusion is that the long-run behaviour of NGASUS is decoupled from the rest of energy prices.

Remember that, according to Theorem 3, the univariate estimation in CiSSA of an oscillatory

component at a certain frequency of a time series is the sum of the 9 subcomponents associated to this frequency in the multivariate M-CiSSA setup. If the number of subcomponents to practically pick up the total variability of the long-run behaviour of the individual series is less than the total number of series, then there are common long-run trends. Disentangling what is common and what is idiosyncratic to each series is the value added of the multivariate M-CiSSA approach. In Figure 2 we show for each series its univariate trend as well as the trend coming from the first subcomponent. The first thing to notice is the high resemblance between the first subcomponent and the trend for all the commodities except for NGASUS, that is in line with the percentage of explained variability shown in Table 4 for each series by this first subcomponent. Understanding the first subcomponent as the main common driver of the evolution of the prices, shows how NGASUS presents a differentiated or decoupled evolution from the rest of the energy commodities in the long run.

Figure 2. Trend of the series and estimated first subcomponent.

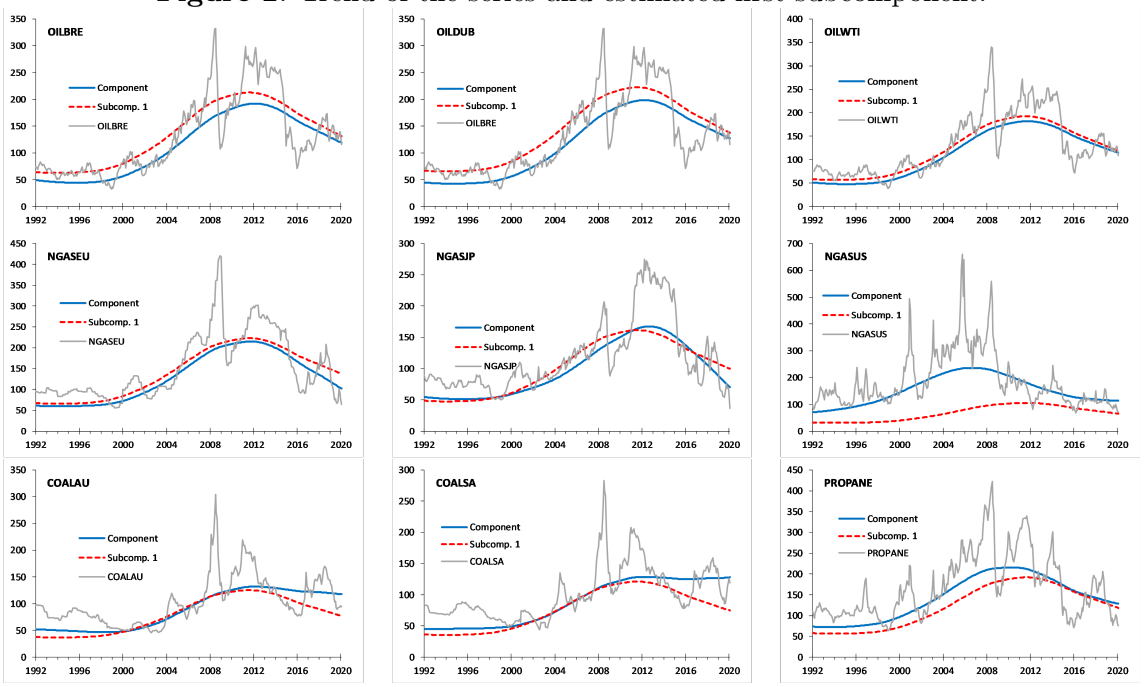

Looking at the first row of Table 4, we note that the first subcomponent is representing a high percentage of the variability, over 92% for all the energy commodities but for NGASUS that stands only for 28.2%. When taking into consideration the first and the second subcomponents, they can explain all the variability.

The multivariate approach also enables us to observe the following behaviours that cannot be derived from univariate analyses. Notice that the sum of the first two long-run subcomponents practically reproduces the univariate trend for each series (see Figure 3). However, we can also observe the following facts: First, the differences in OIL prices, NGASUS and PROPANE between the trend and

Subcomponent	COALAU	COALSA	OILBRE	OILDUB	OILWTI	NGASEU	NGASJP	NGASUS	PROPANE
Trend									
1	92.7	93.8	98.8	98.4	99.9	99.4	92.7	28.2	93.5
2	98.0	98.2	99.9	99.9	100.0	99.5	98.5	99.8	99.5
Cycle									
1	43.2	49.0	95.1	95.1	98.4	90.9	67.5	16.0	90.6
2	76.0	76.1	99.4	99.4	99.4	93.2	87.6	97.1	95.3
3	99.3	98.9	99.5	99.5	99.5	96.5	97.7	99.7	97.4

Table 4. Accumulated contribution of the subcomponents of each series over the variability of the trend and 8-year cycle.

the sum of the first and second subcomponents are negligible. Second, there are some noticeable differences between them for the rest of commodities. In this sense, for COALAU and COALSA we could identify that their price is higher than what the global markets for energy would suggest, meaning that there is something idiosyncratic to their markets that increases their prices. For instance, there are subsidies to coal, trade barriers and even anti-climate change policies that might be responsible for this higher than expected prices. Further research would be needed in order to identify the precise causes of these increases. Third, we can identify 2013 as the year where the discrepancy between the expected global price and the actual trend that they exhibit have increased steadily. Fourth, although in most of the sample the same behaviour can be observed for the Japanese gas (NGASJP), in this case, the behaviour has been inverted rather than getting more acute as it had happened with coal. Fifth, gas in Europe (NGASEU) exhibits the opposite behaviour. The signal extracted by M-CiSSA is a little bit higher than the long-run price that comes from the univariate analysis. In this case, this might be due to the European policy of installing LNG (liquid natural gas) reserves.

3.2 Cyclical behaviour

The second component in relevance is the 96-month, 8-year, cycle that is represented by the second 9×9 block for $k = 2$ of the cross spectral density. Within the 20.3% of variability explained by this cycle (Table 1), it is mainly described by the three first eigenvalues that account for 98.5% (Table 2). Therefore, we are going to analyse the first three eigenvectors to understand the drivers of this 8-year cycles for these 9 series. Within the variability linked to the cycle, the first eigenvalue explains 68.3% of the common variability of the 8-year cycle. Relative weights in Table 3 shows that the first eigenvector is mainly dominated by NGASEU, PROPANE and the three oil prices (OILBRE, OILDUB and OILWTI). Figure 4 shows the segments of the first eigenvector corresponding to each commodity. Despite their amplitudes already commented we can also see the cyclical position of each

Figure 3. Trend of the series and sum of the estimated first and second subcomponents.

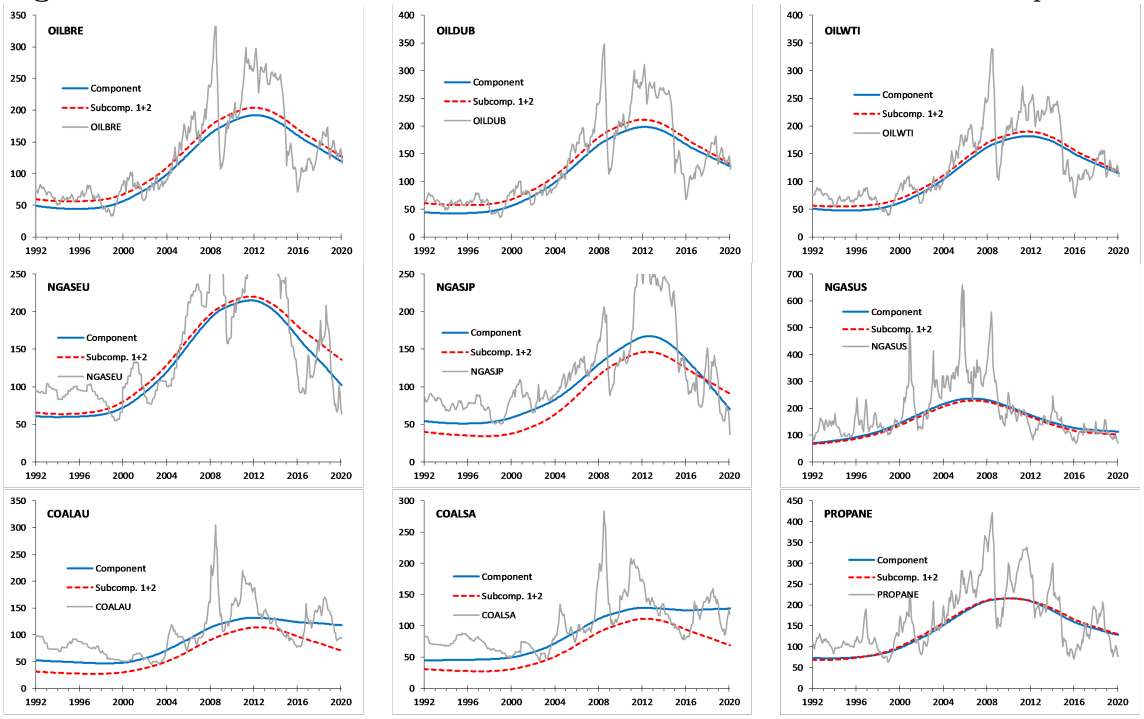

series with respect to the others. We can see that oil prices (OILBRE, OILDUB OILWTI) co-move also with NGASEU, while coals (COALAU, COALSA) and PROPANE seem slightly leading and NGASUS is completely decoupled. The second eigenvalue explains 26.5% of the common variability of the 8-year cycle. The amplitude of the wave NGASUS is much higher than the rest of the commodities with a relative weight of 67.9%. The cyclical position is again completely decoupled with respect to the remaining commodities. Finally, within the third eigenvalue the highest amplitudes of the waves correspond to NGASJP and the two coals (COALAU, COALSA). We also see that the two coals are in phase while NGASJP shows an anticyclical behaviour with respect to them. This is the reason why, despite the small variability explained by this third eigenvalue (3.7%), the segments of the eigenvector are necessary to understand the behaviour of the prices of the coal market and NGASJP.

Table 4 shows the relative variability explained by each subcomponent in each series at different frequencies. While in the long run we see a decoupling between NGASUS and the rest of the commodities, in the 8-year cycles, COALS and to a less extent NGASJP do also decouple from the remaining commodity prices. Therefore the multivariate analysis by frequencies allows to further understand price market co-movements.

Figure 4. Eigenvector segments for each variable of the 8-year cycle.

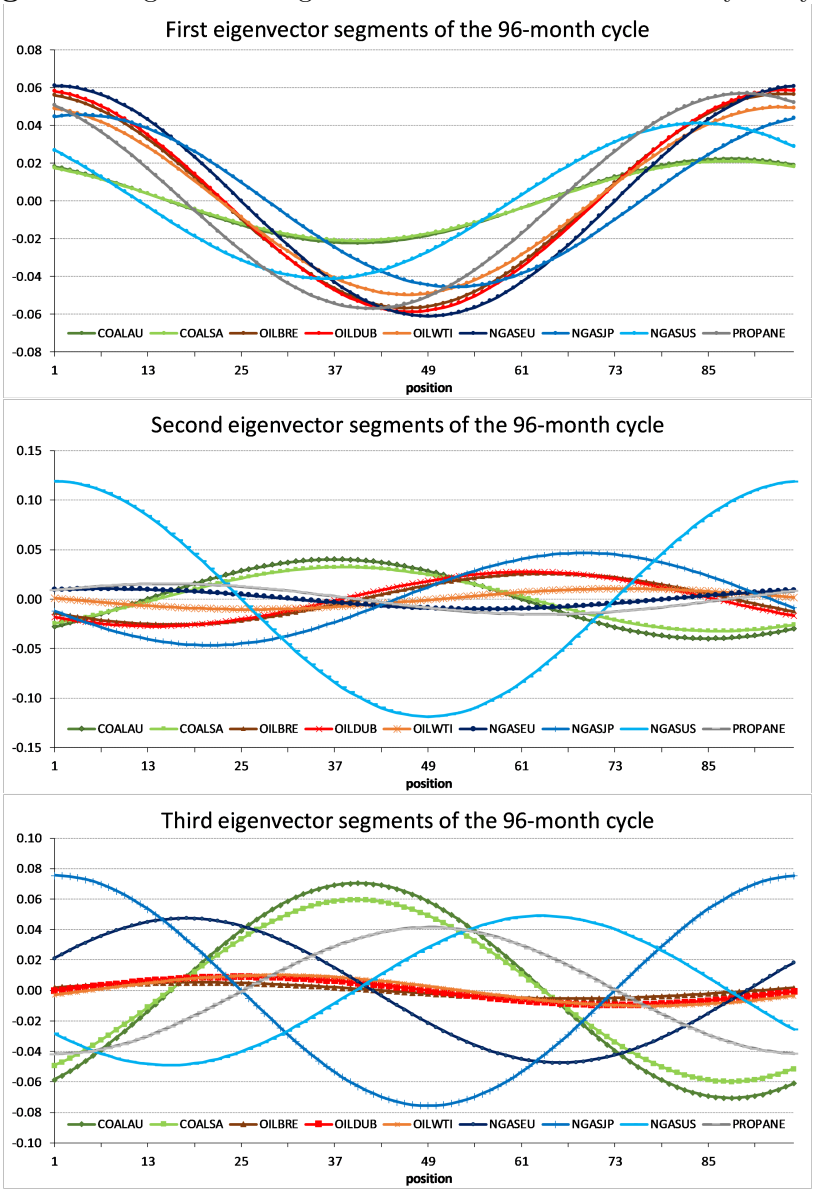

4 Concluding Remarks

We have introduced a new methodology that allows to disentangle common and idiosyncratic fluctuations within a group of time series by frequency. The methodology is non-parametric and it is a new version of multivariate SSA. SSA algorithms are based on the spectrum (in an algebraic sense) of eigenvalues in a singular value decomposition of a covariance matrix. One of the main problems of preceeding alternatives is the need of identifying each extracted underlying signal with a specific frequency. This is precisely the advantage of circulant SSA.

The multivariate nature of our approach allows also to disentangle which fluctuations are common and which ones are idiosyncratic by frequency. In our case, this is key in order to identify common and specific forces in commodity markets. Additionally, we prove the uniqueness of each extracted

component per frequency, that is, the extracted components in a univariate fashion coincide with the sum of all subcomponents for each frequency extracted in a multivariate way. The value added of the multivariate approach is the ability to disentangle what is common from what is idiosyncratic. This cannot be done with the univariate approach since there is no information regarding what is common.

As we do not need to specify a model to extract the different components, the approach is robust to misspecifications. The only parameter we need to choose before applying the methodology is L, the window length.

We have applied M-CiSSA to energy commodity prices. These series are key for medium and lon-term energy policy issues. In particular, we find the nature of decoupling at different frequencies. In this regard, we find that US natural gas is decoupled both at low as well as at the cyclical frequency although this is not the case for all the series. Coals are decoupled for the cyclical frequency while they co-move in the long run. This is precisely one novelty of our approach: we can check at what frequencies markets are decoupled. We are also able to analyze the relative position among the series. Taken as reference the three oils (OILBRE, OILDUB and OILWTI), we detect that the gas in Europe (NGASEU) is in phase with them while coals and propane seem slightly leading. As mentioned before NGASUS is completely decoupled.

The comparison between results in the univariate and multivariate cases also allows to discover which prices are held or sustained by forces outside the global evolution of the markets. In particular for the long run, we find that although coals are not decoupled, their prices are higher than suggested by the global forces of the markets. We also find that long-run prices for natural gas in Europe, NGASEU, exhibit a lower level than suggested, probably due to the European policy of installing of LNG (liquid natural gas) reserves.

Finally, our approach is quite general and it can be applied to many disciplines involving analyzing time series. Among other things, it can be used to separate long, medium and short-run analysis, cyclical analysis, forecasting scenarios, denoising time series and extracting common from idiosyncratic signals by frequency due to the ability of the procedure to extract signals at the desired frequencies specified by the user. All this is done without modeling the time series since we only need to select the window length L.

References

[1] International Energy Agency (2019). *World energy prices: An overview.* Available at https://webstore.iea.org/world-energy-prices-2019-an-overview

[2] United Nations (2015). *Transforming our world: The 2030 Agenda for Sustainable Development.* United Nations.

[3] European Commission (2019). *The European Green Deal, Communication from the Commission to the European Parliament, The European Council, the Council, the European Economic and social Committee and the Committee of the Regions.* European Commission. December 2019.

[4] Krätschell, K. and Schmidt, T. (2017). Long-run waves or short-run fluctuations- what establishes the correlation between oil and food prices. *Applied Economics*, 49 (54), 5535-5546.

[5] Xu, Y., Wan, L. and Yin, L. (2019). Dynamic link between oil prices and Exchange rates: A non-linear approach. *Energy Economics*, 84, 104488.

[6] Garratt, A. and Petrella, I. (2019). Commodity prices and inflation risk. *Unpublished*, Warwick.

[7] Alquist, R., Bhattarai, S. and Coibion, O. (2019). Commodity-price co-movement and global economic activity. *Journal of Monetary Economics.* In press.

[8] Kilian, L. and Zhou, X. (2018). Modeling fluctuations in the global demand for commodities. *Journal of International Money and Finance*, 88, 54-78.

[9] Brown, S.P.A. and Yücel, M.K. (2008). What drives natural gas prices? *Energy Journal*, 29, 43–58.

[10] Brown, S.P.A. and Yücel, M.K. (2009). Market arbitrage: European and North American natural gas prices. *Energy Journal*, 30, 167–186.

[11] Erdös, P. (2012). Have oil and gas prices got separated? *Energy Policy*, 49, 707-718.

[12] Nick, S. and Thoenes, S. (2014). What drives natural gas prices? - A structural VAR approach. *Energy Economics*, 45, 517–527

[13] Zhang, D. and Ji, Q. (2018). Further evidence on the debate of oil-gas price decoupling: A long memory approach. *Energy Policy*, 113, 68–75.

[14] Ghil, M., Allen, R.M., Dettinger, M.D., Ide, K., Kondrashov, D., Mann, M.E., Robertson, A., Saunders, A., Tian, Y., Varadi, F. and Yiou, P. (2002). Advanced spectral methods for climatic time series. *Reviews of Geophysics*, 40 (1), 1-41.

[15] Golyandina, N. and Zhigljavsky, A. (2013). *Singular Spectrum Analysis for Time Series.* Springer.

[16] Broomhead, D. and King, G. (1986b). On the qualitative analysis of experimental dynamical systems. In *Nonlinear Phenomena and Chaos*, 113-144. A. Hilger ed., Bristol

[17] Broomhead, D. and King, G. (1986a). Extracting qualitative dynamics from experimental data. *Physica D*, 20, 217-236.

[18] Fraedrich, K. (1986). Estimating the dimension of weather and climate attractors. *Journal of the Atmospheric Sciences*, 43 (5), 419-432.

[19] Plaut, G. and Vautard, R. (1994). Spells of Low-Frequency Oscillations and Weather Regimes in the Northern Hemisphere. *Journal of the Atmospheric Sciences*, 51 (2), 210-236.

[20] Lee, T.K., Gan, S.S., Lim, J.G. and Sanei, S. (2014). A multivariate Singular Spectrum Analysis approach to clinically-motivated movement biometrics. In *Signal Processing Conference (EUSIPCO), Proceedings of the 22nd European*, 1397-1401. IEEE.

[21] Golyandina, N. and Usevich, K.D. (2010). 2D-extension of Singular Spectrum Analysis: algorithm and elements of theory. In *Matrix Methods: Theory, Algorithms and Applications: Dedicated to the Memory of Gene Golub*, 449-473.

[22] Gruszczynska, M., Klos, A., Rosat, S. and Bogusz, J. (2017). Deriving common seasonal signals in GPS position time series by using multichannel singular spectrum analysis. *Acta Geodynamica et Geromaterialia*, 14 (3), 273-285.

[23] Groth, A., Ghil, M., Hallegatte, S. and Dumas, P. (2015). The role of oscillatory modes in US business cycles. *Journal of Business Cycle Measurement and Analysis*, 2015 (1), 63. OCDE.

[24] Hassani, H., Heravi, S. and Zhigljavsky, A. (2013). Forecasting UK industrial production with multivariate singular spectrum analysis. *Journal of Forecasting*, 32 (5), 395-408.

[25] Hassani, H., Soofi, A.S. and Zhigljavsky, A. (2013). Predicting inflation dynamics with singular spectrum analysis. *Journal of the Royal Statistical Society: Series A (Statistics in Society)*, 176 (3), 743-760.

[26] Zhang, J., Hassani, H., Xie, H. and Zhang, X. (2014). Estimating multi-country prosperity index: a two-dimensional singular spectrum analysis approach. *Journal of Systems Science and Complexity*, 27 (1), 56-74.

[27] Sella, L., Vivaldo, G., Groth, A. and Ghil, M. (2016). Economic cycles and their synchronization: a comparison of cyclic modes in three European countries. *Journal of Business Cycle Research*, 12 (1), 25-48.

[28] Silva, E. S., Hassani, H. and Heravi, S. (2018). Modelling European industrial production with multivariate singular spectrum analysis: A cross-industry analysis. *Journal of Forecasting*, 37 (3), 371-384.

[29] Bógalo, J., Poncela, P. and Senra, E. (2020). Circulant Singular Spectrum Analysis: A new automated procedure for signal extraction. *arXiv preprint* arXiv:2003.12859.

[30] Gutiérrez-Gutiérrez, J. and Crespo, P.M. (2008). Asymptotically equivalent sequences of matrices and Hermitian block Toeplitz matrices with continuous symbols: Applications to MIMO systems. *IEEE Transactions on Information Theory*, 54 (12), 5671-5680.

[31] Pearl, J. (1973). On Coding and Filtering Stationary Signals by Discrete Fourier Transform. *IEEE Transactions on Information Theory*, IT-19, 229-232.

[32] Groth, A. and Ghil, M. (2011). Multivariate singular spectrum analysis and the road to phase synchronization. *Physical Review E*, 84 (3), 036206.

[33] Vautard, R., Yiou, P. and Ghil, M. (1992). Singular-spectrum analysis: A toolkit for short, noisy chaotic signal. *Physica D*, 58, 95-126.

[34] Groth, A., Ghil, M., Hallegatte, S. and Dumas, P. (2011). Identification and reconstruction of oscillatory modes in US business cycles using Multivariate Singular Spectrum Analysis. In *Workshop on Frequency Domain Research in Macroeconomics and Finance*. Bank of Finland, Helsinki.

[35] Carvalho, M. de and Rua, A. (2017). Real-time nowcasting the US output gap: Singular spectrum analysis at work. *International Journal of Forecasting*, 33 (1), 185-198.

[36] Peña, D. and Yohai, V.J. (2016). Generalized dynamic principal components. *Journal of the American Statistical Association*, 111(515), 1121-1131.

[37] Allen, M.R. and Robertson, A.W. (1996). Distinguishing modulated oscillations from coloured noise in multivariate datasets. *Climate Dynamics*, 12, 775-784.

[38] Cuddington, J.T. and Nülle, G. (2013). Variable long-term trends in mineral prices: The ongoing tug-of-war between exploration, depletion, and technological change. *Journal of International Money and Finance*, 30, 1-29.

[39] Tilli, P. (1998). Singular values and eigenvalues of non-Hermitian block Toeplitz matrices. *Linear algebra and its applications*, 272 (1-3), 59-89.

A Theorems and Proofs

A.1 Proof of Theorem 1

$\widetilde{\mathbf{F}}$ is a continuous matrix function and $\mathbf{C}_L\left(\widetilde{\mathbf{F}}\right)$ is also a block Toeplitz matrix. It holds that $\sigma_1\left(\mathbf{T}_L\left(\mathbf{F}\right)\right) \leq \sigma_1\left(\mathbf{F}\right) < \infty$ and $\sigma_1\left(\mathbf{C}_L\left(\widetilde{\mathbf{F}}\right)\right) \leq \sigma_1\left(\widetilde{\mathbf{F}}\right) < \infty \quad \forall L \in \mathbb{N}$ [39], where $\sigma_1\left(\mathbf{A}\right)$ is the largest singular value of matrix $\mathbf{A}$. We also must proof that $\lim_{L\to\infty} L^{\frac{-1}{2}} \left\|\mathbf{T}_L\left(\mathbf{F}\right) - \mathbf{C}_L\left(\widetilde{\mathbf{F}}\right)\right\|_F = 0$. From (3) and (6) we have that

$$
\begin{aligned}
&\tfrac{1}{L}\left\|\mathbf{T}_L\left(\mathbf{F}\right) - \mathbf{C}_L\left(\widetilde{\mathbf{F}}\right)\right\|_F^2 \\
&\quad= \sum_{k=1}^{L-1} \tfrac{(L-k)k^2}{L^3}\left(\left\|\mathbf{\Gamma}_k - \mathbf{\Gamma}_{-L+k}\right\|_F^2 + \left\|\mathbf{\Gamma}_{-k} - \mathbf{\Gamma}_{L-k}\right\|_F^2\right) \\
&\quad= \sum_{r=1}^{M}\sum_{s=1}^{N}\sum_{k=1}^{L-1} \tfrac{(L-k)k^2}{L^3}\left(\left|\left[\mathbf{\Gamma}_k\right]_{r,s} - \left[\mathbf{\Gamma}_{-L+k}\right]_{r,s}\right|^2 + \left|\left[\mathbf{\Gamma}_{-k}\right]_{r,s} - \left[\mathbf{\Gamma}_{L-k}\right]_{r,s}\right|^2\right).
\end{aligned}
$$

As $\left[\mathbf{\Gamma}_k\right]_{r,s} \in \mathbb{C}$, we write $\left[\mathbf{\Gamma}_k\right]_{r,s} = a_{k,r,s} + i \cdot b_{k,r,s}$ where $a_{k,r,s}, b_{k,r,s} \in \mathbb{R}$. Therefore,

$$
\begin{aligned}
\sum_{k=1}^{L-1}\left|\left[\mathbf{\Gamma}_k\right]_{r,s} - \left[\mathbf{\Gamma}_{-L+k}\right]_{r,s}\right|^2 &= \sum_{k=1}^{L-1}\left(a_{k,r,s} - a_{-L+k,r,s}\right)^2 + \sum_{k=1}^{L-1}\left(b_{k,r,s} - b_{-L+k,r,s}\right)^2 \\
&= \sum_{k=1}^{L-1} a_{k,r,s}^2 + \sum_{k=1}^{L-1} a_{-L+k,r,s}^2 - 2\sum_{k=1}^{L-1} a_{k,r,s}a_{-L+k,r,s} \\
&\quad + \sum_{k=1}^{L-1} b_{k,r,s}^2 + \sum_{k=1}^{L-1} b_{-L+k,r,s}^2 - 2\sum_{k=1}^{L-1} b_{k,r,s}b_{-L+k,r,s} \\
&= \sum_{k=1}^{L-1}\left|\left[\mathbf{\Gamma}_k\right]_{r,s}\right|^2 + \sum_{k=1}^{L-1}\left|\left[\mathbf{\Gamma}_{-L+k}\right]_{r,s}\right|^2 - 2\sum_{k=1}^{L-1} a_{k,r,s}a_{-L+k,r,s} - 2\sum_{k=1}^{L-1} b_{k,r,s}b_{-L+k,r,s} \quad .
\end{aligned}
$$

Considering that $2|xy| \leq x^2 + y^2 \quad \forall x, y \in \mathbb{R}$, we have that

$$
\begin{aligned}
&\sum_{k=1}^{L-1}\left|\left[\mathbf{\Gamma}_k\right]_{r,s} - \left[\mathbf{\Gamma}_{-L+k}\right]_{r,s}\right|^2 \\
&\quad\leq \sum_{k=1}^{L-1}\left|\left[\mathbf{\Gamma}_k\right]_{r,s}\right|^2 + \sum_{k=1}^{L-1}\left|\left[\mathbf{\Gamma}_{-L+k}\right]_{r,s}\right|^2 + \sum_{k=1}^{L-1}\left(a_{k,r,s}^2 + a_{-L+k,r,s}^2\right) + \sum_{k=1}^{L-1}\left(b_{k,r,s}^2 + b_{-L+k,r,s}^2\right) \\
&\quad= 2\left(\sum_{k=1}^{L-1}\left|\left[\mathbf{\Gamma}_k\right]_{r,s}\right|^2 + \sum_{k=1}^{L-1}\left|\left[\mathbf{\Gamma}_{-L+k}\right]_{r,s}\right|^2\right) \quad .
\end{aligned}
$$

In the same way,

$$
\sum_{k=1}^{L-1}\left|\left[\mathbf{\Gamma}_{-k}\right]_{r,s} - \left[\mathbf{\Gamma}_{L-k}\right]_{r,s}\right|^2 \leq 2\left(\sum_{k=1}^{L-1}\left|\left[\mathbf{\Gamma}_{-k}\right]_{r,s}\right|^2 + \sum_{k=1}^{L-1}\left|\left[\mathbf{\Gamma}_{L-k}\right]_{r,s}\right|^2\right).
$$

As a consequence

$$\begin{aligned}
&\sum_{k=1}^{L-1}\left(\left|[\mathbf{\Gamma}_k]_{r,s}-[\mathbf{\Gamma}_{-L+k}]_{r,s}\right|^2+\left|[\mathbf{\Gamma}_{-k}]_{r,s}-[\mathbf{\Gamma}_{L-k}]_{r,s}\right|^2\right)\\
&\quad\leq 2\left(\sum_{k=1}^{L-1}\left|[\mathbf{\Gamma}_k]_{r,s}\right|^2+\sum_{k=1}^{L-1}\left|[\mathbf{\Gamma}_{-L+k}]_{r,s}\right|^2+\sum_{k=1}^{L-1}\left|[\mathbf{\Gamma}_{-k}]_{r,s}\right|^2+\sum_{k=1}^{L-1}\left|[\mathbf{\Gamma}_{L-k}]_{r,s}\right|^2\right)\\
&\quad=4\left(\sum_{k=-L+1}^{L-1}\left|[\mathbf{\Gamma}_k]_{r,s}\right|^2-\left|[\mathbf{\Gamma}_0]_{r,s}\right|^2\right)\leq 4\sum_{k=-L+1}^{L-1}\left|[\mathbf{\Gamma}_k]_{r,s}\right|^2
\end{aligned}$$

and, therefore,

$$\sum_{k=1}^{L-1}\tfrac{(L-k)k^2}{L^3}\left(\left|[\mathbf{\Gamma}_k]_{r,s}-[\mathbf{\Gamma}_{-L+k}]_{r,s}\right|^2+\left|[\mathbf{\Gamma}_{-k}]_{r,s}-[\mathbf{\Gamma}_{L-k}]_{r,s}\right|^2\right)\leq 4\sum_{k=-L+1}^{L-1}\tfrac{(L-|k|)k^2}{L^3}\left|[\mathbf{\Gamma}_k]_{r,s}\right|^2.$$

Parseval's Theorem guaranties quadratic summability of $\left\{[\mathbf{\Gamma}_k]_{r,s}\right\}_{k\in\mathbb{Z}}$ $\forall\, 1\leq r\leq M$ and $1\leq s\leq N$. So, given $\varepsilon>0$, you can choose $P>0$ big enough such that $\sum_{k=P}^{\infty}\left(\left|[\mathbf{\Gamma}_k]_{r,s}\right|^2+\left|[\mathbf{\Gamma}_{-k}]_{r,s}\right|^2\right)\leq\varepsilon$. Then,

$$\begin{aligned}
&\lim_{L\to\infty}\sum_{k=1}^{L-1}\tfrac{(L-k)k^2}{L^3}\left(\left|[\mathbf{\Gamma}_k]_{r,s}-[\mathbf{\Gamma}_{-L+k}]_{r,s}\right|^2+\left|[\mathbf{\Gamma}_{-k}]_{r,s}-[\mathbf{\Gamma}_{L-k}]_{r,s}\right|^2\right)\\
&\quad\leq 4\lim_{L\to\infty}\sum_{k=-L+1}^{L-1}\tfrac{(L-|k|)k^2}{L^3}\left|[\mathbf{\Gamma}_k]_{r,s}\right|^2\\
&\quad=4\lim_{L\to\infty}\left\{\sum_{k=-P+1}^{P-1}\tfrac{(L-|k|)k^2}{L^3}\left|[\mathbf{\Gamma}_k]_{r,s}\right|^2+\sum_{k=P}^{L-1}\tfrac{(L-k)k^2}{L^3}\left(\left|[\mathbf{\Gamma}_k]_{r,s}\right|^2+\left|[\mathbf{\Gamma}_{-k}]_{r,s}\right|^2\right)\right\}\\
&\quad\leq 4\lim_{L\to\infty}\sum_{k=-P+1}^{P-1}\tfrac{(L-|k|)k^2}{L^3}\left|[\mathbf{\Gamma}_k]_{r,s}\right|^2+4\sum_{k=P}^{\infty}\left(\left|[\mathbf{\Gamma}_k]_{r,s}\right|^2+\left|[\mathbf{\Gamma}_{-k}]_{r,s}\right|^2\right)\leq 0+4\varepsilon=4\varepsilon\ .
\end{aligned}$$

For all this,

$$\begin{aligned}
&\lim_{L\to\infty}\tfrac{1}{L}\left\|\mathbf{T}_L(\mathbf{F})-\mathbf{C}_L\left(\widetilde{\mathbf{F}}\right)\right\|_F^2\\
&\quad=\lim_{L\to\infty}\sum_{r=1}^{M}\sum_{s=1}^{N}\sum_{k=1}^{L-1}\tfrac{(L-k)k^2}{L^3}\left(\left|[\mathbf{\Gamma}_k]_{r,s}-[\mathbf{\Gamma}_{-L+k}]_{r,s}\right|^2+\left|[\mathbf{\Gamma}_{-k}]_{r,s}-[\mathbf{\Gamma}_{L-k}]_{r,s}\right|^2\right)\\
&\quad=\sum_{r=1}^{M}\sum_{s=1}^{N}\lim_{L\to\infty}\sum_{k=1}^{L-1}\tfrac{(L-k)k^2}{L^3}\left(\left|[\mathbf{\Gamma}_k]_{r,s}-[\mathbf{\Gamma}_{-L+k}]_{r,s}\right|^2+\left|[\mathbf{\Gamma}_{-k}]_{r,s}-[\mathbf{\Gamma}_{L-k}]_{r,s}\right|^2\right)\\
&\quad\leq 4MN\varepsilon\,.
\end{aligned}$$

As ε is any number,

$$\lim_{L\to\infty}L^{\frac{-1}{2}}\left\|\mathbf{T}_L(\mathbf{F})-\mathbf{C}_L\left(\widetilde{\mathbf{F}}\right)\right\|_F=0$$

and, therefore, $\mathbf{T}_L(\mathbf{F}) \sim \mathbf{C}_L\left(\widetilde{\mathbf{F}}\right)$.

A.2 Proof of Proposition 2

The solutions on the unit circle of the equation $z^n = 1$ add up to zero and $\mathbf{V}$ is an unitary matrix. Therefore, we have that

$$\begin{aligned}\sqrt{2}\mathcal{R}'_{\mathbf{v}_i}\sqrt{2}\mathcal{R}_{\mathbf{v}_j} &= \tfrac{1}{2}(\mathbf{v}_i+\bar{\mathbf{v}}_i)'(\mathbf{v}_j+\bar{\mathbf{v}}_j) = \tfrac{1}{2}\left[\mathbf{v'}_i\mathbf{v}_j+\mathbf{v}_i^*\mathbf{v}_j+\overline{(\mathbf{v}_i^*\mathbf{v}_j)}+\overline{(\mathbf{v'}_i\mathbf{v}_j)}\right]\\ &= \begin{cases}\tfrac{1}{2}(0+0+0+0)=0 & i\neq j\\ \tfrac{1}{2}(0+1+1+0)=1 & i=j\end{cases},\end{aligned}$$

that

$$\begin{aligned}\sqrt{2}\mathcal{I}'_{\mathbf{v}_i}\sqrt{2}\mathcal{I}_{\mathbf{v}_j} &= \tfrac{-1}{2}(\mathbf{v}_i-\bar{\mathbf{v}}_i)'(\mathbf{v}_j-\bar{\mathbf{v}}_j) = \tfrac{-1}{2}\left[\mathbf{v'}_i\mathbf{v}_j-\mathbf{v}_i^*\mathbf{v}_j-\overline{(\mathbf{v}_i^*\mathbf{v}_j)}+\overline{(\mathbf{v'}_i\mathbf{v}_j)}\right]\\ &= \begin{cases}\tfrac{-1}{2}(0-0-0+0)=0 & i\neq j\\ \tfrac{-1}{2}(0-1-1+0)=1 & i=j\end{cases}\end{aligned}$$

and also that

$$\begin{aligned}\sqrt{2}\mathcal{R}'_{\mathbf{v}_i}\sqrt{2}\mathcal{I}_{\mathbf{v}_j} &= \tfrac{-i}{2}(\mathbf{v}_i+\bar{\mathbf{v}}_i)'(\mathbf{v}_j-\bar{\mathbf{v}}_j) = \tfrac{-i}{2}\left[\mathbf{v'}_i\mathbf{v}_j-\mathbf{v}_i^*\mathbf{v}_j+\overline{(\mathbf{v}_i^*\mathbf{v}_j)}-\overline{(\mathbf{v'}_i\mathbf{v}_j)}\right]\\ &= \begin{cases}\tfrac{-i}{2}(0-0+0-0)=0 & i\neq j\\ \tfrac{-i}{2}(0-1+1-0)=0 & i=j\end{cases}.\end{aligned}$$

Furthermore, since for the eigenvalue-eigenvector pair $(\lambda_{k,m}, \mathbf{v}_{k,m})$ it is held $\mathbf{C}_L(\mathbf{F})\mathcal{R}_{\mathbf{v}_{k,m}} + \mathrm{i}\,\mathbf{C}_L(\mathbf{F})\mathcal{I}_{\mathbf{v}_{k,m}} = \lambda_{k,m}\mathcal{R}_{\mathbf{v}_{k,m}} + \mathrm{i}\,\lambda_{k,m}\mathcal{I}_{\mathbf{v}_{k,m}}$, that is, $\mathbf{C}_L(\mathbf{F})\mathcal{R}_{\mathbf{v}_{k,m}} = \lambda_{k,m}\mathcal{R}_{\mathbf{v}_{k,m}}$ and $\mathbf{C}_L(\mathbf{F})\mathcal{I}_{\mathbf{v}_{k,m}} = \lambda_{L+2-k,m}\mathcal{I}_{\mathbf{v}_{k,m}}$ because $\lambda_k = \lambda_{L+2-k}$, the proposition is proved.

A.3 Proof of Theorem 3

In M-CiSSA, the elementary matrix for the *m-th* subcomponent at frequency ω_k for the *i-th* series, using the unitary matrix $\mathbf{V}$ defined in (9) and following the expression (11), is given by

$$\mathbf{X}_{k,m}^{(i)} = \mathbf{v}_{k,m}^{(i)}\mathbf{v}_{k,m}^*\mathbf{X}\,. \tag{15}$$

The eigenvector $\mathbf{v}_{k,m} = \mathbf{v}_{(k-1)M+m}$ of the unitary matrix $\mathbf{V}$ can be expressed as

$$\mathbf{v}_{k,m} = (\mathbf{U}_L \otimes \mathbf{I}_M)(\mathbf{1}_{M,k} \otimes \mathbf{e}_{k,m})$$

what, together with formula (10), transforms equation (15) into

$$\mathbf{X}_{k,m}^{(i)} = \left(\mathbf{I}_L \otimes \mathbf{1}_{M,i}^T\right) (\mathbf{U}_L \otimes \mathbf{I}_M) \left(\mathbf{1}_{M,k} \otimes \mathbf{e}_{k,m}\right) \left(\mathbf{1}_{M,k} \otimes \mathbf{e}_{k,m}\right)^* (\mathbf{U}_L \otimes \mathbf{I}_M)^* \mathbf{X} \,. \tag{16}$$

Adding the previous equality (16) in m, we obtain that

$$\begin{aligned}
\sum_{m=1}^{M} \mathbf{X}_{k,m}^{(i)} &= \left(\mathbf{I}_L \otimes \mathbf{1}_{M,i}^T\right) (\mathbf{U}_L \otimes \mathbf{I}_M) \left[\sum_{m=1}^{M} \left(\mathbf{1}_{M,k} \otimes \mathbf{e}_{k,m}\right) \left(\mathbf{1}_{M,k} \otimes \mathbf{e}_{k,m}\right)^*\right] (\mathbf{U}_L \otimes \mathbf{I}_M)^* \mathbf{X} \\
&= \left(\mathbf{I}_L \otimes \mathbf{1}_{M,i}^T\right) (\mathbf{U}_L \otimes \mathbf{I}_M) \operatorname{diag}\left(\mathbf{0}, \cdots, \mathbf{I}_M, \cdots, \mathbf{0}\right) (\mathbf{U}_L \otimes \mathbf{I}_M)^* \mathbf{X} \\
&= \mathbf{u}_k \mathbf{u}_k^* \mathbf{X}^{(i)} \\
&= \mathbf{X}_k^{(i)}
\end{aligned}$$

where $\mathbf{X}^{(i)}$ is the trajectory matrix for the *i-th* series and the identity matrix $\mathbf{I}_M$ occupies the *k-th* place in the block diagonal matrix $\operatorname{diag}\left(\mathbf{0}, \cdots, \mathbf{I}_M, \cdots, \mathbf{0}\right)$. Therefore, it is shown that $\sum_{m=1}^{M} \mathbf{X}_{k,m}^{(i)} = \mathbf{X}_k^{(i)}$ and, as a consequence, the oscillatory component of any series for each frequency is unique.